Zwitterionic Ring-Opening Copolymerization of Tetrahydrofuran and Glycidyl Phenyl Ether with B(C6F5)3

ARTICLE *in* MACROMOLECULES · MARCH 2015

Impact Factor: 5.8 · DOI: 10.1021/acs.macromol.5b00096

Macromolecules

Article

pubs.acs.org/Macromolecules

Zwitterionic Ring-Opening Copolymerization of Tetrahydrofuran and Glycidyl Phenyl Ether with $B(C_6F_5)_3$

Isabel Asenjo-Sanz,[†] Antonio Veloso,[‡] José I. Miranda,[§] Angel Alegría,[†,∥] José A. Pomposo,[†,∥,⊥] and Fabienne Barroso-Bujans*[,†,#]

[†]Centro de Física de Materiales (CSIC-UPV/EHU)-MPC, Paseo Manuel Lardizábal 5, San Sebastian 20018, Spain

[‡]POLYMAT and [§]SGIKer, NMR Service, University of the Basque Country UPV/EHU, Joxe Mari Korta R&D Ctr, Avda. Tolosa-72, San Sebastian 20018, Spain

[∥]Departamento de Física de Materiales, University of the Basque Country UPV/EHU, Apartado 1072, San Sebastian 20080, Spain

[⊥]IKERBASQUE-Basque Foundation for Science, María Díaz de Haro 3, Bilbao 48013, Spain

[#]Donostia International Physics Center (DIPC), Paseo Manuel Lardizábal 4, San Sebastian 20018, Spain

Supporting Information

ABSTRACT: This report describes a simple strategy to produce copolymers of tetrahydrofuran (THF) and glycidyl phenyl ether (GPE) by using $B(C_6F_5)_3$ as a catalyst. The control of the synthesis conditions, such as reaction time, catalyst concentration, and monomer concentration, allows the formation of copolymers with molecular weights in the range of 15−330 kg/mol. MALDI-TOF mass spectrometry revealed that with a low THF content in the feed cyclic copolymers are the major reaction products, whereas with a high THF content, linear copolymers are the main products. To explain these results, a zwitterionic ring-opening copolymerization mechanism was postulated based on DFT calculations and experimental results. Physical properties of the resulting copolymers demonstrated that by changing the relative amounts of monomers copolymers with tailored glass transition temperatures in a broad range of temperatures from −84 to −4 °C can be obtained and that crystallization of THF fragments can be suppressed. Rheological measurements showed that by controlling the degree of crystallization, copolymers with rubber-like behavior can be obtained in a broad temperature range below room temperature.

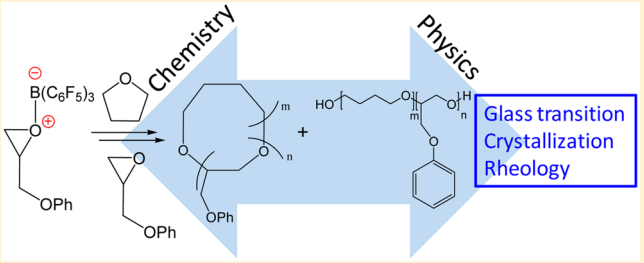

INTRODUCTION

Zwitterionic ring-opening polymerization (ZROP) involves the attack of nucleophiles[1] or electrophiles[2] to strained heterocylic monomers to generate ionic propagating species. The counterion is contained in the same polymer chain. This method has been proved to be effective in the generation of cyclic polymers of high molecular weight.[1] The advantages of this approach lie in the simplicity of the reaction, high reaction conversion, fast reaction time, and the fact that the monomer concentration is not a limiting condition. Cyclic polymers can be obtained at relatively high monomer concentration[1] and even in bulk conditions.[2]

The ZROP of cyclic monomers with nucleophilic catalysts such as N-heterocyclic carbenes,[3,4] amidines,[5] pyridines,[6] tertiary amines,[7] imidazoles,[8] and isothioureas[9] has been comprehensively studied in the past few years. The catalyst mediates the ring-opening of cyclic monomers to form zwitterionic intermediates that propagate and cyclize to produce macrocycles. By means of these synthetic strategies, cyclic polymers such as poly(lactide),[3,4] poly(caprolactone),[10] polypeptides,[7] and poly(carbosiloxane)s[11] as well as gradient copolymers of ε-caprolactone and δ-valerolactone[12] have been obtained. In some cases, contamination with linear homologues has been observed.

Less attention has been paid to ZROP mediated by electrophiles. Very recently, we observed that the electrophilic catalyst, $B(C_6F_5)_3$, reacts with oxirane monomers to produce cyclic polyethers of high molecular weight in anhydrous and bulk conditions.[2] By using this strategy, hydrophilic and hydrophobic cyclic polyethers containing pendant functional groups can be easily synthesized in one step and in high quantities (grams). A ZROP mechanism was postulated to account for the observed experimental evidence, where the catalyst initiates the polymerization by forming an oxirane−$B(C_6F_5)_3$ zwitterion. We note that reaction times in the ZROP of oxirane monomers[2] are much higher than those in the ZROP of lactide and lactones.[1] The former reactions occur in the order of hours whereas the second ones are extremely rapid, occurring in the order of seconds. In addition, in both cases the experimental M_n cannot be predicted from the initial ratio of monomer to initiator ($[M]_0/[I]_0$): in the ZROP of oxirane

Received: January 16, 2015
Revised: February 20, 2015
Published: March 3, 2015

DOI: 10.1021/acs.macromol.5b00096
Macromolecules 2015, 48, 1664−1672

Table 1. Copolymers of Glycidyl Phenyl Ether (GPE) and Tetrahydrofuran (THF) Initiated by $B(C_6F_5)_3$

entry	composition[a]	$[GPE]_0/[THF]_0$ (mol %)	M_n[b] (kg/mol)	M_w/M_n[b]	$[GPE]_0/[B(C_6F_5)_3]_0$ (mol/mol)	reaction time (h)	conversion[c] (%)
1	P(GPE)	100/0	17.4	1.9	943	24	78
2	$P(GPE_{0.80}$-*co*-$THF_{0.20})$	80/20	30.5	1.8	943	3	25
3	$P(GPE_{0.63}$-*co*-$THF_{0.37})$	60/40	35.7	1.8	943	3	22
4	$P(GPE_{0.53}$-*co*-$THF_{0.47})$	37/63	49.6	1.6	943	3	45
5	$P(GPE_{0.35}$-*co*-$THF_{0.65})$	23/77	45.2	1.8	94	3	57
6	$P(GPE_{0.40}$-*co*-$THF_{0.60})$	23/77	93.7	1.6	419	24	70
7	$P(GPE_{0.42}$-*co*-$THF_{0.58})$	23/77	111.4	1.8	539	24	68
8	$P(GPE_{0.34}$-*co*-$THF_{0.66})$	22/78	130.6	1.8	943	22	61
9	$P(GPE_{0.28}$-*co*-$THF_{0.72})$	22/78	175.7	1.8	943	27	62
10	$P(GPE_{0.03}$-*co*-$THF_{0.97})$	2/98	333.0	1.8	471	15	30

[a]Obtained by integration of ^1H NMR signals. [b]Determined by SEC with conventional PS calibration. [c]Obtained by the weight of the precipitated polymers.

monomers, $M_n < [M]_0/[I]_0$, and in the ZROP of lactide, $M_n > [M]_0/[I]_0$. These differences in both polymerization reactions can be attributed to the inherent kinetic characteristics of the catalyst and monomer pair.

Another ring-opening polymerization (ROP) approach is one that combines a Lewis acid, $Zn(C_6F_5)_2$, with bases such as amines and phosphines to promote the ROP of lactide and ε-caprolactone leading to cyclic homopolymers and copolymers.[13] In the presence of THF, the authors found that polytetrahydrofuran (PTHF) was formed as a side product due to the activation of THF by the Lewis pair.[13] It has also been postulated that $B(C_6F_5)_3$ catalyzes the copolymerization reaction of oxirane monomers and vinyl ethers via concurrent cationic vinyl addition and ROP.[14,15] Initiation was hypothesized to take place from the coordination of the catalyst to an oxirane molecule.[15] In the course of our investigations on the ZROP of GPE with $B(C_6F_5)_3$,[2,16] we observed that when THF was used as a solvent, copolymers of high molecular weight were obtained. Given the importance of PTHF in the plastic and synthetic fiber industry, particularly in the technology of polyurethanes, polyesters, and polyamides, we extended our investigation to the study of copolymers of GPE and THF (hereafter P(GPE-*co*-THF)).

PTHF crystallizes near room temperature which complicates its handling in the industry. Copolymerization of THF with a variety of monomers has been used as a strategy to circumvent difficulties associated with crystallization. The presence of comonomers might reduce crystallization and/or the melting temperature of THF polymers[17] as well as improving the mechanical properties of polyurethanes derived from THF-based copolymers.[18] Another advantage of the comonomer is that it introduces antibacterial properties to THF polymers.[19] A variety of advanced materials based on THF polymers have also been reported such as star-shaped polymers,[20] cyclic,[21] multicyclic,[22] and supramolecular structures.[23,24]

It has been well documented that cationic ROP is the only polymerization mechanism available to THF.[25] This has been intensively studied in the past and reviewed in several publications.[25−27] Polymerization of THF proceeds via tertiary oxonium ion associated with a negatively charged counterion. Initiation can occur by alkylation or acylation of the oxygen of THF, by the addition of strong protonic acids, by *in situ* generation of the oxonium ion, by photoinitiation,[28] or by a combination of mechanisms, i.e., the formation of secondary (protonated THF) and tertiary (alkylated THF) oxonium ions.[29] Upon certain conditions, initiation involving secondary and tertiary oxonium ions is relatively slow. The addition to the media of much more reactive oxiranes (epichlorohydrin, ethylene oxide, or propylene oxide)[30,31] considerably increases the rate of initiation. The oxirane is frequently referred to as a promoter.[25]

In the present study, we discuss the results of copolymerization studies of THF and GPE with $B(C_6F_5)_3$. This Lewis acid is able to initiate the copolymerization reaction without the use of any other cocatalyst. We observed by MALDI-TOF mass spectrometry (MS) that at low THF fractions cyclic copolyethers are formed as the major reaction product but that at high THF fractions linear copolyethers are preferentially formed. On the basis of these results and on DFT calculations, we hypothesize that copolymerization of GPE and THF proceeds through a zwitterionic ring-opening copolymerization mechanism, where the oxonium ions of THF and GPE are the active species. Countering the positive charge of the oxirane is an anionic boron center in an $OB(C_6F_5)_3$ fragment. We also found that the molecular weight linearly increases with conversion and that at high THF fractions values as high as 330 kg/mol can be reached. Furthermore, the properties of the resulting copolymer can be tailored by changing the monomer composition and the molecular weight. Copolymers with crystalline and/or amorphous structures as well as with variations of the glass transition temperature (T_g) from −84 to −4 °C can be obtained.

EXPERIMENTAL SECTION

Copolymerization of GPE and THF. Reagents were manipulated and transferred either by distillation or under argon in a vacuum line. GPE and THF (Aldrich) were dried over CaH_2, degassed, and distilled in a vacuum line. $B(C_6F_5)_3$ (Aldrich) was sublimed in vacuum at 50 °C and transferred to the reaction flask in a glovebox. Copolymers of GPE and THF were synthesized at room temperature in bulk conditions. In a typical experiment (entry 9, Table 1), 2 mg of $B(C_6F_5)_3$ (3.9 μmol), 1 mL of THF (12.33 mmol), and 0.5 mL of GPE (3.68 mmol) were added to a Schlenk flask under an argon atmosphere. After 27 h of reaction time, the mixture was dissolved in dichloromethane and precipitated in methanol. As a reference material, poly(glycidyl phenyl ether) [P(GPE)] was synthesized in bulk conditions by reaction of 0.5 mL of GPE with 2 mg of $B(C_6F_5)_3$ at room temperature (entry 1, Table 1). The mixture was stirred for 24 h, subsequently dissolved in dichloromethane, and precipitated in methanol. All samples were dried at 80 °C in a vacuum oven.

Characterization. The molecular weight and molecular weight distribution were determined by size exclusion chromatography (SEC) on an Agilent G-1310A HPLC pump equipped with PLgel 5 μm Guard and PLgel 5 μm Mixed-C columns at a flow rate of 1 mL/min THF. A calibration curve based on linear PS standards was used in

DOI: 10.1021/acs.macromol.5b00096
Macromolecules 2015, 48, 1664−1672

conjunction with a differential refractive index (RI) detector (Optilab rEX, Wyatt).

MALDI-TOF MS measurements were performed on a Bruker Autoflex Speed system (Bruker, Germany) equipped with a 355 nm Nd:YAG laser. Spectra were acquired in the positive reflectron mode. *trans*-2-[3-(4-*tert*-Butylphenyl)-2-methyl-2-propenylidene]malonitrile (DCTB, Fluka) was used as a matrix. Sodium iodide (Aldrich) was added as the cationic ionization agent (~10 mg/mL dissolved in THF). The matrix was also dissolved in THF at a concentration of 20 mg/mL. Copolymers were dissolved in THF at a concentration of ~10 mg/mL. In a typical MALDI experiment, the matrix, salt, and polymer solutions were premixed at a 20:1:3 ratio, respectively. Approximately 0.5 μL of the obtained mixture was spotted by hand on the ground steel target plate. For each spectrum 1000 laser shots were accumulated. Polytools software (Bruker) was used to identify the molecular weight and end-group structure of the polymer chains.

The copolymerization reaction was monitored by quantitative ^{13}C NMR on a Bruker Avance spectrometer at 500 MHz. 0.5 mL of GPE (3.68 mmol), 0.3 mL of THF (3.68 mmol), and 20 mg of $B(C_6F_5)_3$ (39 μmol) were transferred into an NMR tube, which was immediately introduced into the NMR probe at 25 °C. The GPE conversion was calculated from the integrals of epoxide signals at 43 and 49 ppm relative to those of aromatic signals of GPE. The THF conversion was calculated from the integrals of THF signal at 24 ppm relative to those of aromatic signals of GPE. The composition of copolymers was obtained by integration of ^{1}H NMR signals recorded on a Bruker Avance spectrometer at 400 MHz.

DSC measurements were carried out on ~10 mg specimens using a Q2000 TA Instruments machine in standard mode. A helium flow rate of 25 mL/min was used throughout. Measurements were performed by placing the samples in sealed aluminum pans, equilibrating the temperature at 100 °C, cooling to −100 °C at 10 °C/min, and heating back to 100 °C at 10 °C/min. This procedure was repeated once again at the same cooling and heating rates. In the case of semicrystalline copolymers, the samples were molten at 100 °C and subsequently quenched in liquid nitrogen. The quenched samples were then introduced in a previously cooled DSC cell at −150 °C. Then, samples were heated to 100 °C at 10 °C/min, cooled to −150 °C, and heated back to 100 °C at 10 °C/min. The step in heat capacity at the glass transition (ΔC_p), the T_g obtained when ΔC_p is one-half of the total ΔC_p (medium T_g), and a lower bound temperature for the glass-transition range (onset T_g) were evaluated from the total C_p data. The degree of crystallization (χ_c) was obtained from the ratio of the heat of crystallization of THF during cooling (normalized to the THF content in the sample) to the heat of melting of 100% crystalline PTHF, obtained from the ATHAS databank (14.4 kJ/mol).[32]

Rheological measurements were carried out with an ARES-LS2 rheometer, from TA Instruments, with a plate−plate geometry (diameter 25 mm). The sample was maintained under a nitrogen atmosphere, and the temperature was controlled to within ±0.1 °C. Temperature sweep experiments were performed in the linear regime with a shear frequency of 1 Hz. The data were collected using automatically controlled strains from 0.05% (at lower temperatures) to 10% (at higher temperatures). Samples were cooled and heated back at 5 °C/min.

DFT Calculations. DFT calculations were performed by using Gaussian 09.[33] All structures were optimized using the M06 DFT functional, as described by Zhao and Truhlar,[34] and with the triple-ζ, diffuse, polarized 6-311G+(d, p) basis set with the self-consistent reaction field (SCRF). The CPCM solvent model (THF)[35] was used. All calculations were performed with the overall molecular charges being zero (charge = 0) and singlet ground state multiplicities (multiplicity = 1). Electronic energies (not ZPE corrected), enthalpies (298.15 K), and free energies (298.15 K) were obtained from the frequency files under default parameters (details are shown in the Supporting Information).

RESULTS AND DISCUSSION

Synthesis of P(GPE-*co*-THF) Copolymers. Reaction of GPE and THF initiated by $B(C_6F_5)_3$ at room temperature and in bulk conditions leads to the formation of P(GPE-*co*-THF) copolymers. This reaction occurs readily for all the tested initial monomer concentration ratios ($[GPE]_0/[THF]_0$) in both anhydrous and nonanhydrous conditions. For reproducibility of the results, this study was conducted only in anhydrous

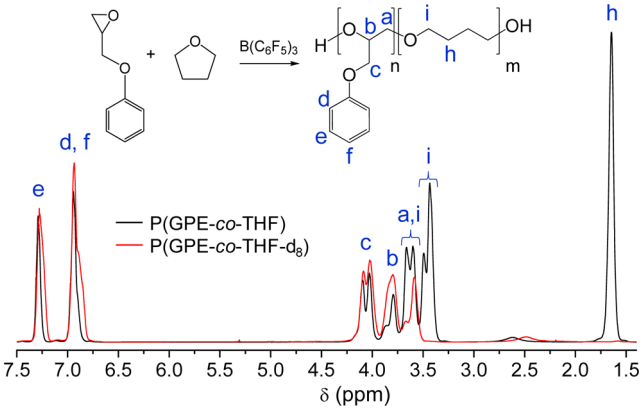

Figure 1. Simplified reaction scheme (for more details see the section about the mechanism of copolymerization) and ^{1}H NMR spectra of P(GPE-*co*-THF) (black) and P(GPE-*co*-THF-d_8) (red) in $CDCl_3$.

conditions. Figure 1 shows a simplified reaction scheme and the ^{1}H NMR spectrum of P(GPE-*co*-THF) obtained at a $[GPE]_0/[THF]_0$ ratio of 37/63 mol % (black line). Signal assignment was performed with the help of edited HSQC and COSY experiments (Figure S1 of the Supporting Information) as well as by registering the ^{1}H NMR spectrum of the copolymer obtained by reaction of GPE and THF-d_8 (P(GPE-*co*-THF-d_8)) (red line). In the latter, the signals corresponding to THF moieties disappear, allowing a clearer interpretation of the spectra. Integration of "h" signals (4H, THF) and that of "e, f, d" signals (5H, GPE) were used to calculate the composition of the synthesized copolymers. The composition, molecular weight, and polydispersity index (PDI) of the synthesized P(GPE-*co*-THF) copolymers are shown in Table 1.

The molecular weight of copolymers synthesized at $[GPE]_0/[THF]_0$ ratios of 23/77 and 2/98 mol % was observed to increase linearly with conversion (Figure 2), indicating a continuous incorporation of both monomers into the growing polymer chain. Copolymers obtained from the mixture containing a larger fraction of THF (98 mol %) showed larger molecular weights at identical conversion as those containing a lower fraction of THF (77 mol %). This result suggests that the incorporation of THF in the growing chain might be faster than that of GPE. To verify if this is the case, the consumption of each monomer was monitored by means of ^{13}C NMR as a function of time. In this experiment, 50/50 mol % $[GPE]_0/[THF]_0$ was used. The data of Figure 3 show that THF is consumed over a 1 h period to reach 94% consumption while GPE reaches only 69% consumption within the same period of time.

If we calculate the theoretical molecular weight by using eq 1

$$M_n = \frac{p_{GPE} M_{GPE} [GPE]_0 + p_{THF} M_{THF} [THF]_0}{[I]_0} \quad (1)$$

DOI: 10.1021/acs.macromol.5b00096
Macromolecules 2015, 48, 1664−1672

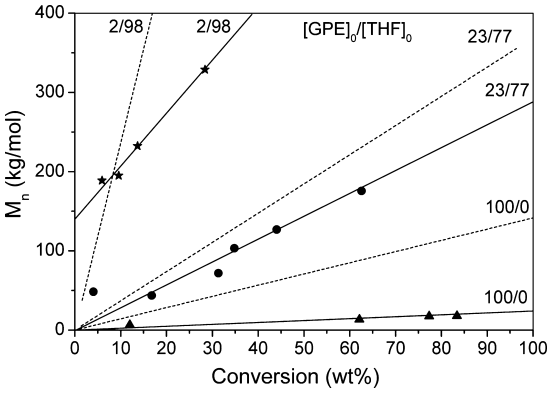

Figure 2. Molecular weight as a function of conversion for copolymers synthesized from 23/77 and 2/98 mol % $[GPE]_0/[THF]_0$ and for the GPE homopolymer (100/0 mol % $[GPE]_0/[THF]_0$). Dashed lines are theoretical molecular weights calculated from eq 1. M_n was determined by SEC. Conversion was determined by the weight of the precipitated polymers.

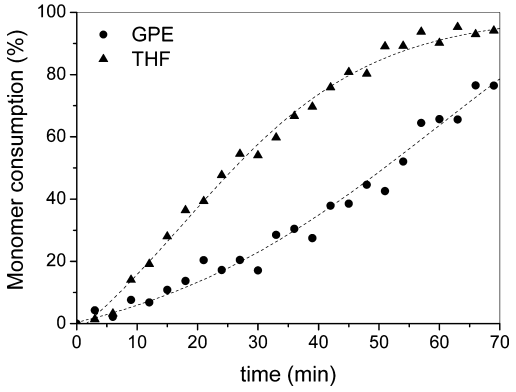

Figure 3. Monomer consumption in the copolymerization reaction catalyzed by $B(C_6F_5)_3$. Data obtained by *in situ* monitoring of the copolymerization by quantitative ^{13}C NMR (see the Experimental Section). Bulk conditions, 50/50 mol % $[GPE]_0/[THF]_0$, $[GPE]_0/[B(C_6F_5)_3]_0$ = 94 mol/mol.

where p_{GPE} and p_{THF} are the fractional conversion of each monomer, obtained from Figure 3, M_{GPE} and M_{THF} are the molecular weights of each monomer, and $[GPE]_0$, $[THF]_0$, and $[I]_0$ are the initial molar concentrations of each monomer and the initiator, respectively, we observe that the experimental M_n values deviate from the computed lines (Figure 2). This is also the case for the GPE homopolymer (100/0 mol % $[GPE]_0/[THF]_0$). In addition, in the case of copolymers obtained from 2/98 $[GPE]_0/[THF]_0$, the nonzero intercept suggest that, in this case, the rate of propagation is faster than that of initiation.[36] These results seem to indicate that the mechanism mediating in the polymerization is strongly dependent on the relative amounts of monomers in the reaction mixture and that transfer might affect the polymerization reaction.

To improve polymerization control in systems dominated by transfer, it has been suggested that the initiator concentration is increased.[36] With this aim, we studied the copolymerization of GPE and THF starting from 23/77 mol % $[GPE]_0/[THF]_0$ at different initiator concentrations. The SEC traces and the molecular weight of the synthesized copolymers as a function of the initial monomer to initiator concentration ratio ($[GPE]_0/[I]_0$ and $[THF]_0/[I]_0$) are shown in Figures 4a and 4b. The data show unimodal molecular weight distributions for all the copolymers and a linear increase of the M_n with both $[GPE]_0/[I]_0$ and $[THF]_0/[I]_0$. As expected from eq 1, by increasing the amount of initiator, the molecular weights of the obtained copolymer were found to decrease. These values, although approximate to the theoretical ones, still show a slight deviation as observed by the lower slope when compared to the diagonal line (Figure 4c).

Mechanism of Copolymerization. To gain further insight into the mechanism of copolymerization of GPE and THF initiated by $B(C_6F_5)_3$, we first analyzed the chemical structure of P(GPE-*co*-THF) copolymers by MALDI-TOF MS. With this aim, two representative copolymer samples containing low and high THF fraction in the copolymer (F_{THF} = 0.20 and 0.87, respectively) were analyzed. The polymerization time was kept low in order to be able to produce polymers with molecular weights below the upper limit of detectable molecular weights by MALDI-TOF MS. The spectrum of the sample with F_{THF} = 0.20 (Figure 5a) revealed well-resolved signals for Na-complexed cyclic $(GPE)_n-(THF)_1$ copolymer chains (red) and cyclic $(GPE)_n$ homopolymer chains (blue). Moreover, an enlarged area of this spectrum (Figure 5b) revealed signals for Na-complexed cyclic $(GPE)_n-(THF)_2$ and cyclic $(GPE)_n-(THF)_3$ copolymer chains (green and pink, respectively). Note that signals identified by the same color are separated by 150 Da (the molecular weight of GPE monomer) and those of different successive color (e.g., from blue to red) by 72 Da (the molecular weight of THF). We found that the signal intensity

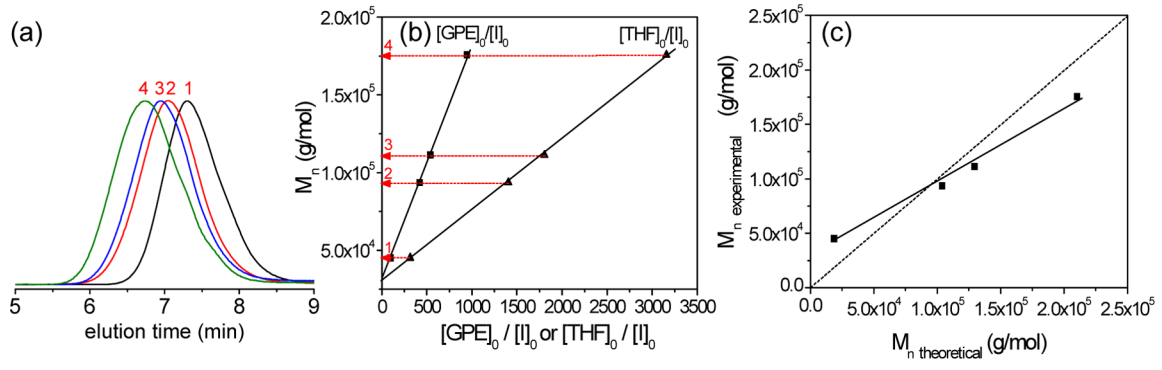

Figure 4. (a) SEC traces of P(GPE-*co*-THF) obtained from 23/77 mol % $[GPE]_0/[THF]_0$ at different initial monomer to initiator concentration ratios ($[GPE]_0/[I]_0$ and $[THF]_0/[I]_0$), polymers denoted as 1–4. In all cases, the conversion was 70 wt %. (b) M_n of polymers 1–4 as a function of $[GPE]_0/[I]_0$ and $[THF]_0/[I]_0$. (c) Comparison of experimental M_n data to those obtained theoretically from eq 1.

DOI: 10.1021/acs.macromol.5b00096
Macromolecules 2015, 48, 1664–1672

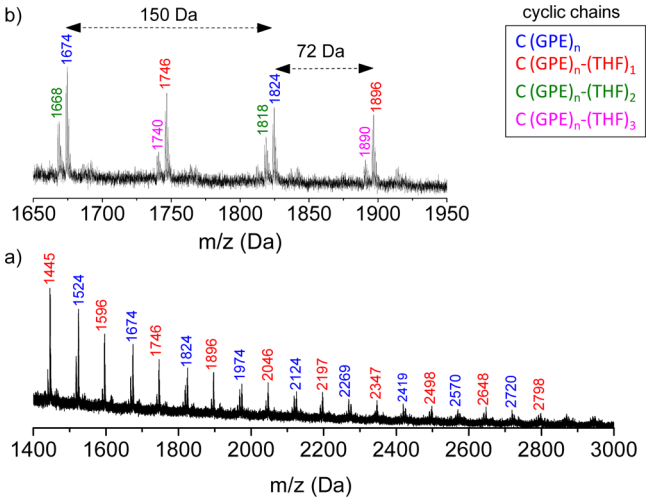

Figure 5. (a) MALDI-TOF MS spectrum of P(GPE-*co*-THF) obtained from 80/20 mol % $[GPE]_0/[THF]_0$ and 1 h reaction time. THF fraction in the copolymer (F_{THF}) = 0.20. (b) Enlarged area of spectrum (a). Na-complexed cyclic (C) chains of $(GPE)_n-(THF)_m$ specimens with m values from 0 to 3 are identified with colors.

decreased with the amount of THF in the copolymer chains. Detection of cyclic $(GPE)_n-(THF)_m$ chains with $m \geq 4$ was not possible for this sample. In contrast to the results obtained for the copolymer synthesized with F_{THF} = 0.20, the MALDI-TOF MS spectrum of the sample with F_{THF} = 0.87 (Figure 6)

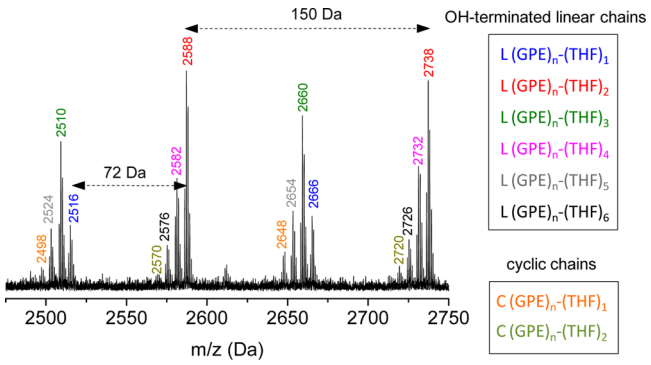

Figure 6. MALDI-TOF MS spectrum of P(GPE-*co*-THF) obtained from 22/78 mol % $[GPE]_0/[THF]_0$ and 0.5 h reaction time. THF fraction in the copolymer (F_{THF}) = 0.87. Na-complexed cyclic (C) chains and Na-complexed OH-terminated linear (L) chains of $(GPE)_n-(THF)_m$ specimens are identified with colors.

revealed that OH-terminated linear chains are the major components. In this case, signals of Na-complexed linear $(GPE)_n-(THF)_m$ chains with m values from 1 to 6 are the most intense of the spectrum. Additionally, small-intensity signals of Na-complexed cyclic $(GPE)_n-(THF)_m$ copolymer chains with m = 1 and 2 are also detected.

To explain the results shown above, we have to invoke a mechanism of reaction where zwitterions are the active species (Scheme 1). Initiation occurs by reaction of $B(C_6F_5)_3$ with both monomers, GPE and THF, leading to the formation of zwitterions Z^1_{GPE} and Z^1_{THF}, respectively. Relative enthalpy energies at 298.15 K ($\Delta H_{298.15}$) of the stabilized Z^1_{GPE} and Z^1_{THF} structures obtained by DFT calculations revealed low-energy intermediates: −10.43 and −13.91 kcal/mol for Z^1_{GPE} and Z^1_{THF}, respectively. These values suggest that Z^1_{GPE} is less stable than Z^1_{THF} and, therefore, that Z^1_{GPE} is more reactive than Z^1_{THF}. On the basis of these results and on unsuccessful attempts to homopolymerize Z^1_{THF} with $B(C_6F_5)$, we propose that Z^1_{GPE} is the active species mediating chain growth. It should be noted that $B(C_6F_5)_3$ forms stable adducts with THF but that in the presence of phosphorus-based nucleophiles the THF is ring-opened to form zwitterionic products containing one or two THF molecules.[37,38] In our experiments we observed that the mere presence of 2 mol % of GPE in the reaction medium is enough to promote the formation of a high molecular weight copolymer rich in THF monomers. Therefore, GPE can be considered a promoter of the initiation process of the polymerization of THF. GPE reacts quickly with $B(C_6F_5)_3$ to create highly reactive zwitterionic species that can be attacked by THF.

Homopropagation of Z^1_{GPE} leads to the formation of Z^n_{GPE} macrozwitterions and to the formation of cyclic P(GPE), as observed by MALDI-TOF MS (Figure 5). Cross-propagation leads to the formation of macrozwitterions $Z(^n_{GPE+}{}^m_{THF})^{GPE}$ and $Z(^n_{GPE+}{}^m_{THF})^{THF}$. Termination can occur by cyclization, which leads to cyclic copolymers (Scheme 1). It can also occur by the addition of water traces or by transfer, which lead to linear copolymers. Both factors will clearly affect the mechanism of reaction: the relative amount of each macrozwitterion and the reactivity of macrozwitterions toward propagation. The first one probably depends on the monomer fraction in the feed and the second one on the macrozwitterion stability. On the basis of these ideas and on MALDI-TOF MS results, it is likely that in the presence of an excess of GPE, $Z(^n_{GPE+}{}^m_{THF})^{GPE}$ is preferentially formed and that this macrozwitterion is prone to termination by cyclization. Likewise, in the presence of an excess of THF, $Z(^n_{GPE+}{}^m_{THF})^{THF}$ is preferentially formed. This macrozwitterion would be prone to propagation by addition of THF. As a result, the molecular weight considerably increases, probably resulting in fewer reactions between the zwitterionic chain ends belonging to the same chain and, therefore, in an increase in the fraction of linear chains in the sample.

Thermal Behavior and Crystallization. DSC study of P(GPE-*co*-THF) samples and their corresponding homopolymers, P(GPE) and PTHF, revealed important thermal characteristics of this sample family. Figure 7 shows the DSC data of representative copolymer samples. Table 2 summarizes the thermal properties of all samples investigated. First of all, the data show that P(GPE) is completely amorphous, but PTHF is semicrystalline at room temperature. Second, the T_g of both homopolymers is separated by approximately 95 °C. And third, the thermal behavior of copolymers varies with the monomer composition, as expected from the combination of thermal properties of both components, GPE and THF.

DSC curves in Figure 7 show that copolymers present only one T_g and that this decreases with the amount of THF in the copolymer. At low amounts of THF (upper panel) the copolymers are completely amorphous, and the T_g range broadens with the increase of THF in the copolymer. At F_{THF} of 0.72 (bottom panel), the copolymer shows pronounced cold crystallization and melting peaks at the temperatures signaled in the figure as T_c and T_m, respectively. The glass transition of the amorphous part of this copolymer can be observed as a broadly extended step. With a further increase of THF in the copolymer, namely F_{THF} = 0.97, T_g and T_c decrease and T_m increases. In this case, the T_g of the amorphous regions becomes narrower and approximates that of PTHF.

DOI: 10.1021/acs.macromol.5b00096
Macromolecules 2015, 48, 1664−1672

Scheme 1. Proposed Mechanism for the Zwitterionic Ring-Opening Copolymerization of GPE and THF with $B(C_6F_5)_3$

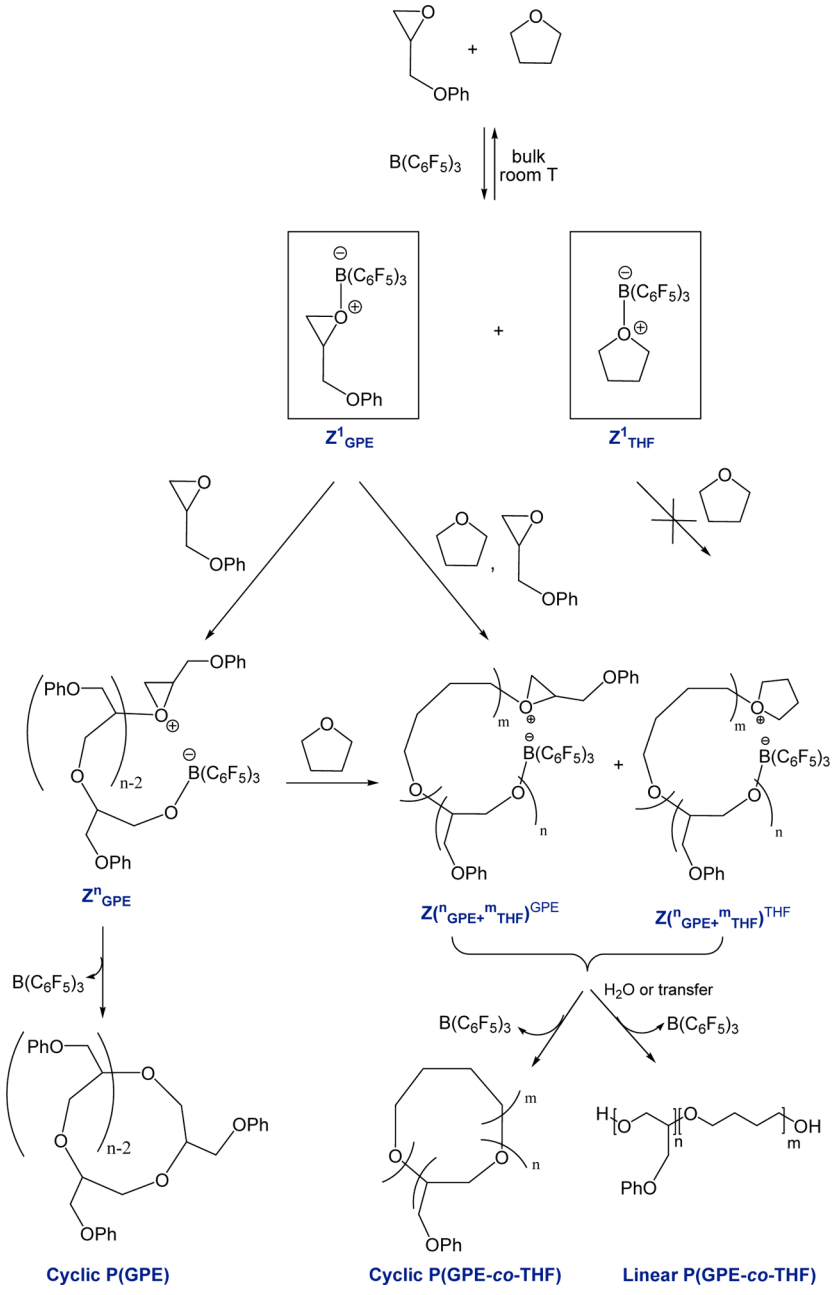

It is worth mentioning that the sample corresponding to entry 8, Table 2, shows no sign of crystallization when cooled at 10 °C/min, but when cooled at 5 °C/min, a broad and small intensity cold crystallization peak appears followed by a melting peak. Under these cooling conditions, the sample reached an extremely low degree of crystallization of only 0.4% (Table 2), but with a relevant impact in the mechanical properties as detailed in the next section. The results suggest that the lower limit for crystallization is with an amount of ∼66 mol % of THF in the copolymer. As the amount of THF in the copolymer increases, higher degrees of crystallization are obtained up to a maximum value of 27%, in agreement with the literature[26] and with the degree of crystallization obtained for PTHF (25%).

Figure 8 shows the dependence of T_g and ΔC_p, obtained by DSC, on the weight fraction of THF (W_{THF}). The T_g data show a composition dependence that can not be described by the Fox equation,[39] but that is well described by the concentration power extended Gordon−Taylor equation.[40] Whereas the former equation predicts the glass transition temperature from data of pure components, the latter equation takes into account the effects of the sequence distribution on the T_g, such as the heterodiads and heterotriads. Therefore, the results seem to indicate that P(GPE-*co*-THF) copolymers deviate from the ideal behavior proposed in the Fox equation to behave as a system where interactions between the different monomeric units of the copolymer play an important role in thermal properties. In this copolymer series it is not obvious how the presence of cyclic chains affects the thermal properties. For instance, according to previous theoretical[41] and experimental work,[42] we might infer that the observed T_g of copolymers with high GPE content is higher than those expected if no cyclic chains were present in the sample. However, in the range of

DOI: 10.1021/acs.macromol.5b00096
Macromolecules 2015, 48, 1664−1672

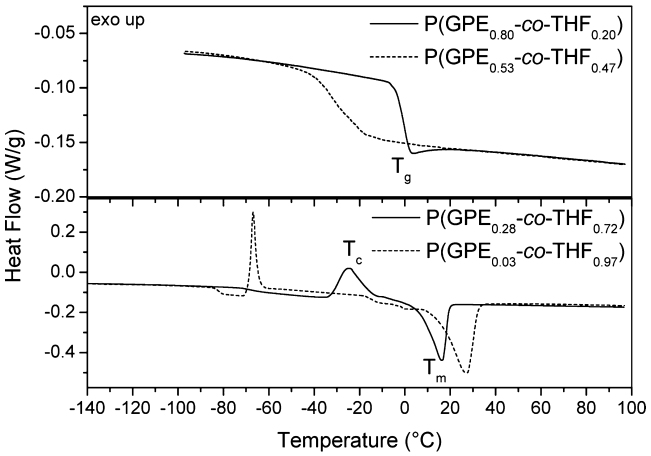

Figure 7. DSC data of representative copolymer samples obtained upon heating at 10 °C/min. Samples in the upper (bottom) panel are the entries 2 and 4 (9 and 10) of Table 2. Samples in the bottom panel were quenched in nitrogen liquid from the melt.

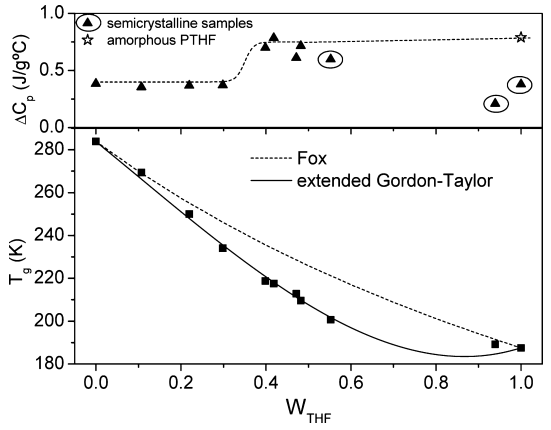

Figure 8. Variation of ΔC_p (top) and T_g (bottom) with the weight fraction of THF in the copolymer (W_{THF}). Top: ΔC_p for completely amorphous bulk PTHF was obtained from the ATHAS databank (57.0 J/(K mol)).[32] Bottom: the lines denote data from the Fox equation[39] and the concentration power extended Gordon−Taylor equation.[40]

molecular weight of the studied samples (M_n > 17 kg/mol) we do not expect a significant effect of cyclization on the T_g.

The ΔC_p data in Figure 8 show nonmonotonous behavior with composition, with a step at about 0.4W_{THF}, to values close to completely amorphous PTHF. As expected from the semicrystalline nature of copolymers with higher THF fraction, these samples present noticeably reduced ΔC_p values.

Rheological Properties. To gain further insights into the effects of crystallization on the properties of the copolymers, four representative samples were characterized by rheology: an amorphous copolymer and its semicrystalline homologous sample, both containing similar monomer composition but different molecular weights (entries 5 and 8, Table 2) and two semicrystalline samples with different degrees of crystallinity (entries 9 and 10, Table 2). The rheological measurements of the storage component of the shear modulus (G') at a single frequency are shown in Figure 9. The amorphous sample (entry 5) shows the characteristic glass to rubber transition at the calorimetric T_g, followed by a further reduction of G' above −20 °C due to the so-called terminal relaxation. In the semicrystalline samples, the glass to rubber transition is much more extended and an additional step at the melting temperature is clearly observed. Interestingly, the sample having only 0.4% χ_c (entry 8) presents a large temperature range of constant G' above T_g. This rubber-like plateau accounts for the presence of small PTHF crystalline regions that act as anchorage points for the amorphous chains, preventing the viscous flow that can be achieved only after melting. The presence of this plateau is less evident for samples with a higher crystallinity (entry 9), and it is not detectable for the most crystalline sample (entry 10).

Concerning the influence of cyclic chains on the rheological properties of the copolymers, it is worth mentioning that the studied samples are mostly linear with a high content of THF and with a high molecular weight. Therefore, we expect that the effects of cyclic chains on the rheological properties are negligible. Furthermore, in the studied range of copolymer composition, the rheological properties are more critically affected by the PTHF crystallization than by the presence of cyclic contaminants.

CONCLUSIONS

This report describes a convenient synthesis of THF-based copolymers by using $B(C_6F_5)_3$ as a catalyst. THF copolymerizes with GPE in a broad range of compositions leading to high molecular weight copolymers in the M_n range of 15−330 kg/mol. A zwitterionic ring-opening copolymerization mecha-

Table 2. Thermal Properties of Copolymers of Glycidyl Phenyl Ether (GPE) and Tetrahydrofuran (THF) and Their Corresponding Homopolymers

entry	composition	onset T_g (°C)	medium T_g (°C)	ΔC_p (J/g°C)	T_c[a] (°C)	T_m (°C)	χ_c[b] (%)
1	P(GPE)	10.7	13.4	0.385			
2	P($GPE_{0.80}$-co-$THF_{0.20}$)	−3.8	−0.7	0.354			
3	P($GPE_{0.63}$-co-$THF_{0.37}$)	−23.2	−19.1	0.368			
4	P($GPE_{0.53}$-co-$THF_{0.47}$)	−39.1	−30.2	0.372			
5	P($GPE_{0.35}$-co-$THF_{0.65}$)	−60.4	−45.7	0.612			
6	P($GPE_{0.40}$-co-$THF_{0.60}$)	−55.6	−39.0	0.785			
7	P($GPE_{0.42}$-co-$THF_{0.58}$)	−54.4	−38.3	0.70			
8	P($GPE_{0.34}$-co-$THF_{0.66}$)	−63.5[c]	−45.9[c]	0.717	broad (−15 to −3)[d]	9.8[d]	0.4
9	P($GPE_{0.28}$-co-$THF_{0.72}$)	−72.5[c]	−68.9[c]	0.60	−24.8[c]	16.1[c]	16
10	P($GPE_{0.03}$-co-$THF_{0.97}$)	−83.9[c]	−82.5[c]	0.21	−66.9[c]	27.5[c]	27
11	PTHF[e]	−85.6[c]	−83.0[c]	0.38	−63.0[c]	19.9[c]	25

[a]Cold-crystallization temperature (T_c). [b]Degree of crystallinity obtained from samples cooled at 5 °C/min. [c]Obtained from samples quenched in liquid nitrogen. [d]Obtained from sample cooled at 5 °C/min. [e]Purchased from Sigma-Aldrich, M_n = 20 kg/mol.

DOI: 10.1021/acs.macromol.5b00096
Macromolecules 2015, 48, 1664−1672

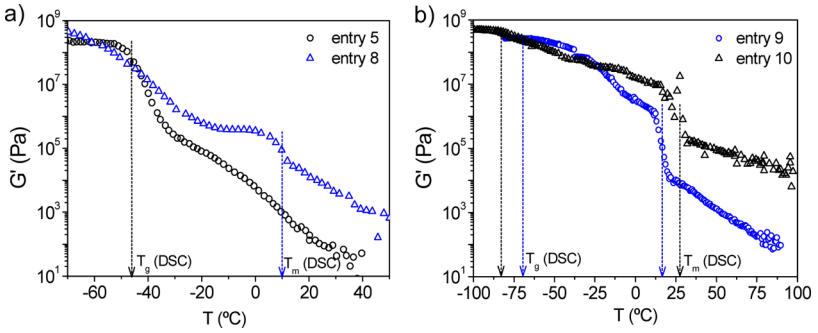

Figure 9. Effect of temperature on the storage modulus of four representative P(GPE-*co*-THF) samples. Samples corresponding to entries 5 and 8 (a) and to entries 9 and 10 (b) of Table 2. Data registered during heating runs at 5 °C/min. T_m and medium T_g of the samples obtained by DSC are indicated in the figures.

nism is proposed, based on DFT calculations and the following experimental evidence. Copolymers obtained from higher THF fractions reach higher molecular weights at a similar conversion. The molecular weight increases linearly with conversion but deviates from the theoretical curves, suggesting that transfer reactions might affect the growing chains. At THF fractions as high as 97 mol % a nonzero intercept is obtained, suggesting that the rate of propagation is faster than that of initiation and that the mechanism mediating in the polymerization is strongly dependent on the relative amounts of monomers in the reaction mixture. The kinetics study by quantitative ^{13}C NMR accounted for a faster consumption of THF than that of GPE in a reaction with equivalent molar ratios of THF and GPE. MALDI-TOF MS data of copolymers obtained from 20 mol % fraction of THF revealed the formation of cyclic copolymers as well as cyclic homopolymer of GPE. When the fraction of THF increased to 78 mol %, then linear copolymers were mainly obtained. To explain all of these results, the formation of zwitterionic species of different reactivity toward propagation and termination is invoked.

The thermal behavior of copolymers can be tailored by simply changing their composition and molecular weight, which can be attained by changing the reaction conditions such as the reaction time, and the concentration of monomers and initiator. By increasing the amount of GPE, the copolymer is totally amorphous, whereas by increasing the amount of THF, the copolymer becomes semicrystalline. The glass transition temperature is largely affected by the monomer composition showing a maximum difference of T_g of 95 °C. The dependence of the T_g on the copolymer composition was well-described by an extended Gordon−Taylor equation, which takes into account the sequence distribution of the monomers in the copolymer, but it could not be described by the Fox equation, which assumes volume additivity of the monomers. Moreover, we found that by controlling the degree of crystallization in the copolymer, by changing either the copolymer composition or the molecular weight, copolymers with rubber-like behavior can be obtained in a broad temperature range below room temperature.

■ ASSOCIATED CONTENT

Supporting Information

Edited HSQC and COSY spectra of P(GPE-*co*-THF) and computational details. This material is available free of charge via the Internet at http://pubs.acs.org.

■ AUTHOR INFORMATION

Corresponding Author

*E-mail fbarroso@ehu.es; Tel +34 94301 8803; Fax +34 94301 5800 (F.B.-B.).

Notes

The authors declare no competing financial interest.

■ ACKNOWLEDGMENTS

We gratefully acknowledge support from MINECO (MAT2012-31088, CTQ2011-25572), Basque Government (IT-654-13, GVIT373-10), Diputación Foral de Gipuzkoa (2011-CIEN-000085-01), University of the Basque Country (UFI 11/56), and Fundación Domingo Martínez (Ayudas a la investigación, 2012). Technical and human support provided by NMR facility and IZO-SGI, SGIker (UPV/EHU, MICINN, GV/EJ, ERDF and ESF), is also acknowledged.

■ REFERENCES

(1) Brown, H. A.; Waymouth, R. M. *Acc. Chem. Res.* **2013**, *46*, 2585−2596.
(2) Asenjo-Sanz, I.; Veloso, A.; Miranda, J. I.; Pomposo, J. A.; Barroso-Bujans, F. *Polym. Chem.* **2014**, *5*, 6905−6908.
(3) Jeong, W.; Shin, E. J.; Culkin, D. A.; Hedrick, J. L.; Waymouth, R. M. *J. Am. Chem. Soc.* **2009**, *131*, 4884−4891.
(4) Culkin, D. A.; Jeong, W.; Csihony, S.; Gomez, E. D.; Balsara, N. P.; Hedrick, J. L.; Waymouth, R. M. *Angew. Chem., Int. Ed.* **2007**, *46*, 2627−2630.
(5) Brown, H. A.; De Crisci, A. G.; Hedrick, J. L.; Waymouth, R. M. *ACS Macro Lett.* **2012**, *1*, 1113−1115.
(6) Kricheldorf, H. R.; Lomadze, N.; Schwarz, G. *Macromolecules* **2007**, *40*, 4859−4864.
(7) Kricheldorf, H. R.; Von Lossow, C.; Schwarz, G. *J. Polym. Sci., Part A: Polym. Chem.* **2006**, *44*, 4680−4695.
(8) Kricheldorf, H. R.; Lomadze, N.; Schwarz, G. *Macromolecules* **2008**, *41*, 7812−7816.
(9) Zhang, X.; Waymouth, R. M. *ACS Macro Lett.* **2014**, *3*, 1024−1028.
(10) Brown, H. A.; Xiong, S.; Medvedev, G. A.; Chang, Y. A.; Abu-Omar, M. M.; Caruthers, J. M.; Waymouth, R. M. *Macromolecules* **2014**, *47*, 2955−2963.
(11) Brown, H. A.; Chang, Y. A.; Waymouth, R. M. *J. Am. Chem. Soc.* **2013**, *135*, 18738−18741.
(12) Shin, E. J.; Brown, H. A.; Gonzalez, S.; Jeong, W.; Hedrick, J. L.; Waymouth, R. M. *Angew. Chem., Int. Ed.* **2011**, *50*, 6388−6391.
(13) Piedra-Arroni, E.; Ladaviere, C.; Amgoune, A.; Bourissou, D. *J. Am. Chem. Soc.* **2013**, *135*, 13306−13309.
(14) Kanazawa, A.; Kanaoka, S.; Aoshima, S. *J. Am. Chem. Soc.* **2013**, *135*, 9330−9333.

DOI: 10.1021/acs.macromol.5b00096
Macromolecules 2015, 48, 1664−1672

(15) Kanazawa, A.; Kanaoka, S.; Aoshima, S. *Macromolecules* **2014**, *47*, 6635−6644.
(16) Perez-Baena, I.; Barroso-Bujans, F.; Gasser, U.; Arbe, A.; Moreno, A. J.; Colmenero, J.; Pomposo, J. A. *ACS Macro Lett.* **2013**, *2*, 775−779.
(17) Liu, L.; Jiang, B.; Zhou, E. *Polymer* **1996**, *37*, 3937−3943.
(18) Clark, A. J.; Hoong, S. S. *Polym. Chem.* **2014**, *5*, 3238−3244.
(19) Theiler, S.; Hövetborn, T.; Keul, H.; Möller, M. *Macromol. Chem. Phys.* **2009**, *210*, 614−630.
(20) Van Renterghem, L. M.; Goethals, E. J.; Du Prez, F. E. *Macromolecules* **2005**, *39*, 528−534.
(21) Oike, H.; Mouri, T.; Tezuka, Y. *Macromolecules* **2001**, *34*, 6592−6600.
(22) Sugai, N.; Heguri, H.; Ohta, K.; Meng, Q.; Yamamoto, T.; Tezuka, Y. *J. Am. Chem. Soc.* **2010**, *132*, 14790−14802.
(23) Beck, J. B.; Ineman, J. M.; Rowan, S. J. *Macromolecules* **2005**, *38*, 5060−5068.
(24) Sivakova, S.; Bohnsack, D. A.; Mackay, M. E.; Suwanmala, P.; Rowan, S. J. *J. Am. Chem. Soc.* **2005**, *127*, 18202−18211.
(25) Pruckmayr, G.; Dreyfuss, P.; Dreyfuss, M. P. Polyethers, Tetrahydrofuran and Oxetane Polymers. In *Kirk-Othmer Encyclopedia of Chemical Technology*; John Wiley & Sons, Inc.: New York, 2000.
(26) Dreyfuss, P. *Poly(tetrahydrofuran)*; Gordon and Breach: London, 1982.
(27) Dreyfuss, P.; Dreyfuss, M. P. Polytetrahydrofuran. In *Fortschritte der Hochpolymeren-Forschung*; Springer: Berlin, 1967; Vol. *4/4*, pp 528−590.
(28) Rodrigues, M. R.; Neumann, M. G. *J. Polym. Sci., Part A: Polym. Chem.* **2001**, *39*, 46−55.
(29) Bednarek, M.; Kubisa, P.; Penczek, S. *Macromolecules* **1999**, *32*, 5257−5263.
(30) Saegusa, T.; Matsumoto, S. *Macromolecules* **1968**, *1*, 442−445.
(31) Bednarek, M.; Biedron, T.; Kubisa, P.; Penczek, S. *Makromol. Chem., Macromol. Symp.* **1991**, *42*−*43*, 475−487.
(32) http://www.springermaterials.com/docs/athas/fulltext/athas00650.html.
(33) Frisch, M. J.; Trucks, G. W.; Schlegel, H. B.; Scuseria, G. E.; Robb, M. A.; Cheeseman, J. R.; Scalmani, G.; Barone, V.; Mennucci, B.; Petersson, G. A.; Nakatsuji, H.; Caricato, M. Li, X.; Hratchian, H. P.; Izmaylov, A. F.; Bloino, J.; Zheng, G.; Sonnenberg, J. L.; Hada, M.; Ehara, M.; Toyota, K.; Fukuda, R.; Hasegawa, J.; Ishida, M.; Nakajima, T.; Honda, Y.; Kitao, O.; Nakai, H.; Vreven, T.; Montgomery, J. A., Jr.; Peralta, J. E.; Ogliaro, F.; Bearpark, M.; Heyd, J. J.; Brothers, E.; Kudin, K. N.; Staroverov, V. N.; Kobayashi, R.; Normand, J.; Raghavachari, K.; Rendell, A.; Burant, J. C.; Iyengar, S. S.; Tomasi, J.; Cossi, M.; Rega, N.; Millam, N. J.; Klene, M.; Knox, J. E.; Cross, J. B.; Bakken, V.; Adamo, C.; Jaramillo, J.; Gomperts, R.; Stratmann, R. E.; Yazyev, O.; Austin, A. J.; Cammi, R.; Pomelli, C.; Ochterski, J. W.; Martin, R. L.; Morokuma, K.; Zakrzewski, V. G.; Voth, G. A.; Salvador, P.; Dannenberg, J. J.; Dapprich, S.; Daniels, A. D.; Farkas, Ö.; Foresman, J. B.; Ortiz, J. V.; Cioslowski, J.; Fox, D. J. *Gaussian09, Revision D.01*; Gaussian Inc.: Wallingford, CT, 2009.
(34) Zhao, Y.; Truhlar, D. G. *Acc. Chem. Res.* **2008**, *41*, 157−167.
(35) Cossi, M.; Rega, N.; Scalmani, G.; Barone, V. *J. Comput. Chem.* **2003**, *24*, 669−681.
(36) Matyjaszewski, K. *J. Phys. Org. Chem.* **1995**, *8*, 197−207.
(37) Welch, G. C.; Masuda, J. D.; Stephan, D. W. *Inorg. Chem.* **2006**, *45*, 478−480.
(38) Birkmann, B.; Voss, T.; Geier, S. J.; Ullrich, M.; Kehr, G.; Erker, G.; Stephan, D. W. *Organometallics* **2010**, *29*, 5310−5319.
(39) Fox, T. G. *Bull. Am. Phys. Soc.* **1956**, *1*, 123−128.
(40) Schneider, H. A.; Rieger, J.; Penzel, E. *Polymer* **1997**, *38*, 1323−1337.
(41) Di Marzio, E. A.; Guttman, C. M. *Macromolecules* **1987**, *20*, 1403−1407.
(42) Clarson, S. J.; Dodgson, K.; Semlyen, J. A. *Polymer* **1985**, *26*, 930−934.

DOI: 10.1021/acs.macromol.5b00096
Macromolecules 2015, 48, 1664−1672